Synthesis of the Pt/C for fuel cell application and Scale-up

by

Hemant Kumar Jaiswal
30EE21J26005

Report of the Major project submitted to the
Academy of Scientific & Innovative Research
for the award of the degree of
MASTER OF TECHNOLOGY

in

ENGINEERING SCIENCES

Under the supervision of
Dr. Amol A Kulkarni

CSIR-National Chemical Laboratory, Pune

Academy of Scientific and Innovative Research
AcSIR Headquarters, CSIR-HRDC campus
Sector 19, Kamla Nehru Nagar,
Ghaziabad, UP – 201 002, India

October - 2022

Content

Certificate

This is to certify that the work incorporated in this M.Tech thesis entitled __**"Synthesis of the Pt/C for fuel cell application and Scale-up"**___ submitted by Mr./Ms. __ **Hemant Kumar Jaiswal**__ to Academy of Scientific and Innovative Research (AcSIR) in fulfilment of the requirements for the award of the Degree of _***Master of Technology***___, embodies original research work under my/our supervision/guidance. I/We further certify that this work has not been submitted to any other University or Institution in part or full for the award of any degree or diploma. Research material obtained from other sources has been duly acknowledged in the thesis. Any text, illustration, table etc., used in the thesis from other sources, have been duly cited and acknowledged.

It is also certified that this work done by the student, under my supervision, is plagiarism free.

Hemant

(Signature of Student)

Hemant Kumar Jaiswal

Enrolment number: 30EE21J26005

Division: CEPD

31/10/2022

(Signature of Supervisor)

Dr. Amol A Kulkarni

ABSTRACT

Name of the Student: Hemant Kumar Jaiswal **Registration No.:** 30EE21J26005

Faculty of Study: Dr. Amol A Kulkarni **Year of Submission:** 2022

AcSIR academic center/CSIR Lab: CSIR-National Chemical Laboratory, Pune

Name of the Supervisor: Dr. Amol A Kulkarni

Title of the thesis: Synthesis of the Pt/C for fuel cell application and Scale-up

---

Emissions of CO2 and other toxic gases are a significant cause of pollution, as transportation contributed immensely due to its dependency on fossil fuels. PEM fuel cells can be a better alternative to fossil fuels because no pollutants are a by-product. Nowadays, increasing demand affects increase the catalyst demand. Catalyst production should be large-scale to fulfill the current and future demand. The catalyst significantly affects the durability and performance of the PEM fuel cell. Synthesis of the catalyst. We have tried reproducing and scaling up the Pt/Vulcan Carbon XC-72. We also attempted to quantify the functional group presented on the carbon surface after the functionalization. The reaction samples were characterized by UV-Vis spectroscopy, TGA, HRTEM, Electrochemical analysis (half-cell), XRD, and BET surface area. We have got the ~38 % Pt loading, Pt particle size - 2.273 ± 0.464 nm, BET surface area - 144.116 m^2/g, and ~75 m^2/g_{Pt} from the 166 mg batch, whereas ~39 % Pt loading, Pt particle size - 2.311±0.470 nm, BET surface area - 140.979 m^2/g, ~70 m^2/g_{Pt} from the 1 gm batch. Results showed that they successfully scaled up by 6-fold.

List of the Figures:

List of the Tables:

Chapter - 1
Introduction

1.1 Motivation:

In the century of changing the energy sector from non-renewable to renewable sources, hydrogen is one of the most famous among the top alternatives of this sector. Almost every country in this world agreed to decrease the CO2 reduction coming years in several meetings because CO2 emission leads to global warming, and now the whole world is facing the scarcity of weather changes. Many serious meetings and commitments happened in the last 2-4 decades. Now, countries are agreed to look for all possible ways to go for alternative sources. India has also committed to the world forum to achieve a 50% CO_2 reduction by 2030 and net Zero by 2070 [1].

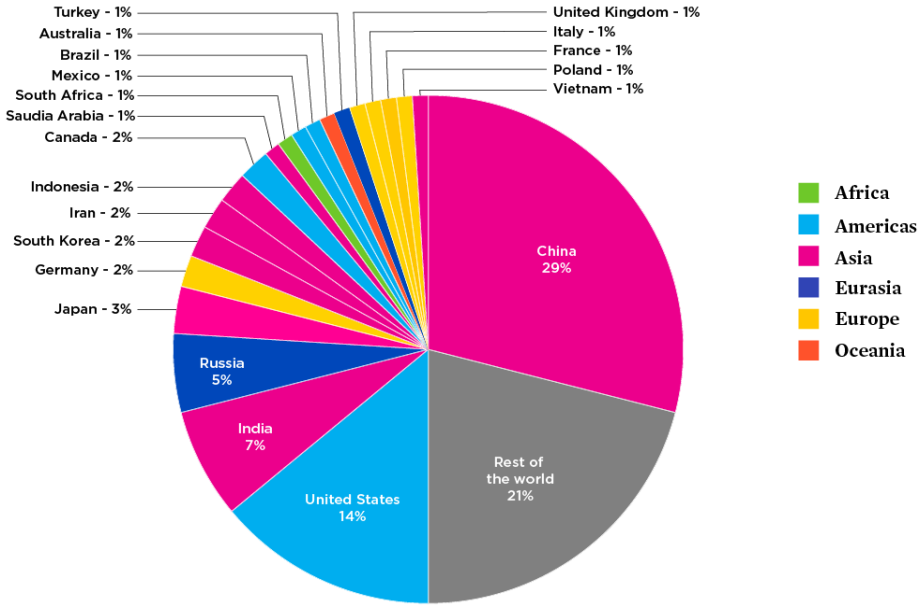

Figure 1 - Countries with the highest annual CO2 emissions in 2019 (from fossil fuels) [2]

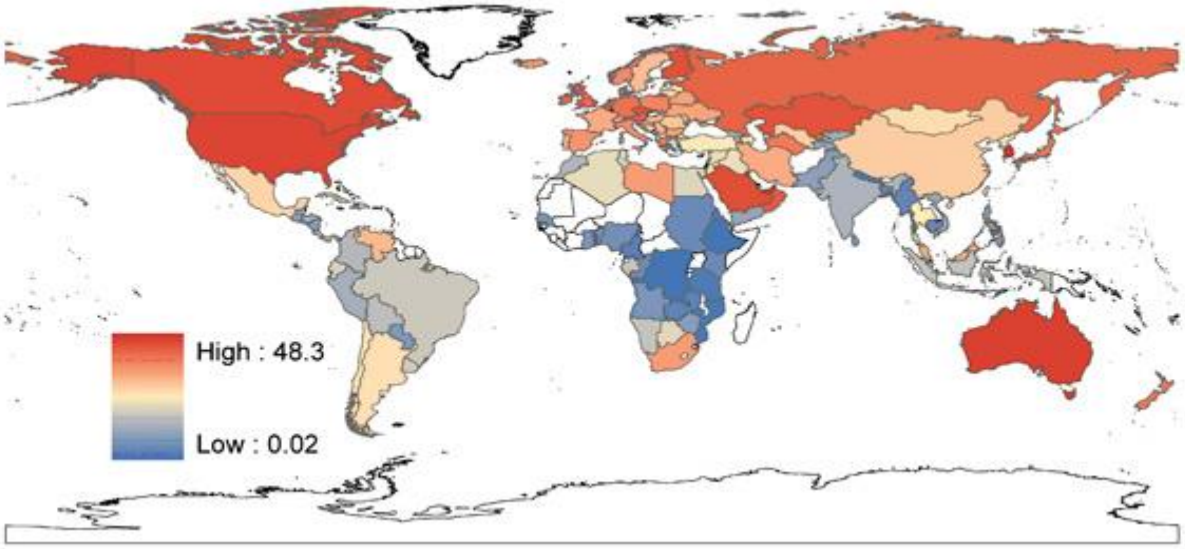

Figure 2 – The national average per capita CO_2 emissions [3]

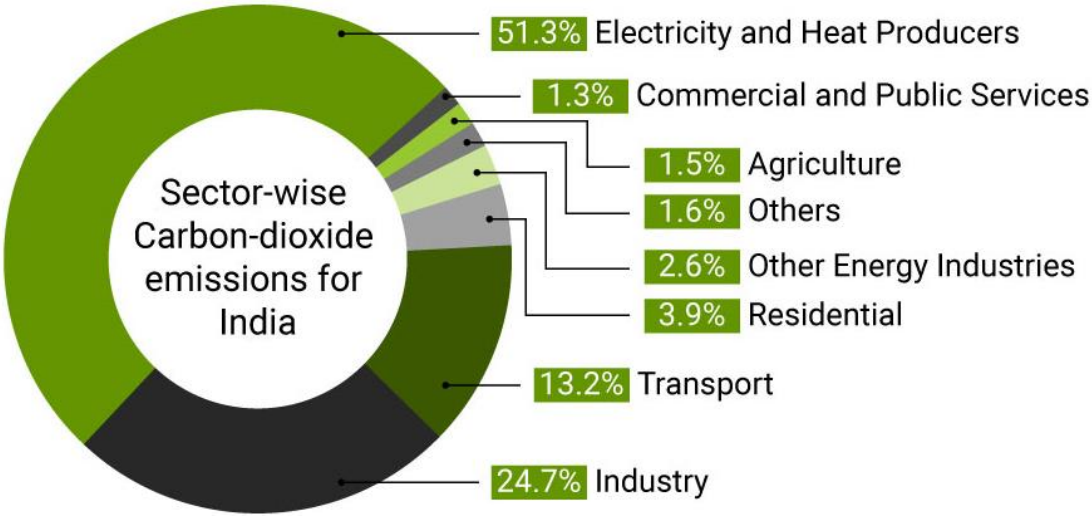

Figure 3 – India's sector-specific CO2 emission share [4]

Several industrial and social sectors are causing CO_2 production due to the majorly using fossil fuels. One of the significant CO_2 production causes is transportation, as in *figure 3*. Transportation is one of the backbone sectors of any country. It helps to transport logistics and people from one part to another within or outside the country.

Countries should look for a better alternative to fossil fuels with lesser pollutant emissions to achieve CO_2 reduction. There are several applicants for renewable and clean energy source as Hydrogen, Solar energy, Hydro energy, Nuclear energy, Geothermal energy, wind energy, etc.

Among all the renewable and clean energy sources, hydrogen is the most suitable alternative and replaceable of fossil fuels in the transportation sector. In this view, the Government of India has also declared the Hydrogen mission programs to be self-reliant in the energy sector and decrease CO_2 production in the coming years [1].

1.2 Advantages and interest in the PEM fuel cell –

Proton Exchange Membrane (PEM) Fuel Cell is one of the alternatives in the transportation sector which use hydrogen as fuel because of its several advantages as [5]:

1. Quick start-up
2. No CO_2 emission is purely working on hydrogen
3. High energy density over other fuel cells
4. Can use air as an oxidant for the ORR
5. Low-temperature operation (60℃ - 80℃)
6. Easy to maintain

1.3 PEM Fuel Cell operating conditions –

- **Temperature** – 60℃ - 80℃
- **Pressure** – 0 - 2 bar back pressure (gauge)
- **Flow rate** – based on the consumption (current)

- **Air flow** – Compressor or blower
- **Temperature control** – Air Cooled or Liquid Cooled
    - **Till 1 - 1.5 kW** FC stack – Stacked can be **air cooled**
    - **>1.5 kW** FC stack– Stacked should be cooled by **liquid** as air cooling is not proper (Liquid should be an Electrical insulator and high heat capacity, generally used water)
- Need **Humidifier** for incoming H2 and Air – Nafion only conduct proton in wet condition

One of the most crucial parts of the PEMFC is its catalyst because of its high cost [6]. Since the Important metal, platinum is precious and costly, we only think of looking for cheaper support and a cheaper synthesis process.

1.4 Application of the PEM fuel cell with the level of power

***Table 1* –** Application of the Fuel cell with its level of power [7]

Level of power	Applications
>1 MW	Local distributed power station
100 kW–1 MW	(1) Large transportation vehicles, such as naval ships, submarines, and buses; (2) Small portable power station; and (3) Small stationary power station
10 kW–100 kW	(1) Transportation vehicles such as cars and mid-size buses; (2) Backup power for mid-size communication station; and (3) Small power station
1 kW–10 kW	(1) Transportation vehicles such as motorcycles, utility vehicles, cars, yachts; (2) Various portable power devices used for field working, underwater platform; and (3) Backup power; uninterruptible power, residential power system
100 W–1 kW	(1) Simple riding devices such as bicycles, scooters, and wheelchairs; Backpack power; (2) Power for exhibition or demonstration; (3) UPS for small services, terminals, and computers
10 W–100 W	(1) Portable power such as for emergency working power supply and military equipment; (2) Battery replacements; (3) Lighting; (4) Signal light power; and (5) Laptop computers
<10 W	(1) Small portable power device; (2) Cell phone

Chapter - 2
Literature Review

2.1 Fuel cell basic mechanisms:

Fuel cells have various kinds based on the chemicals used to generate electricity through electrochemical reactions. Generally, there is reduction at the cathode and oxidation at the anode. In the PEM fuel cell, hydrogen comes in the anode side, where its oxidation occurs. The H+ ion is transferred to the Cathode side by specifically designed PEM, and the electron is transported through the outer electrical circuit. When an electron and an H+ ion from the anode side are present, reduction occurs at the cathode as oxygen from the stack's outer side is adsorbed on the catalyst's active sites. H_2O formed as a product on the anode, as shown in *figure 4* [8], [9]. The major problem of the PEM fuel cell is the sluggish oxygen reduction rate.

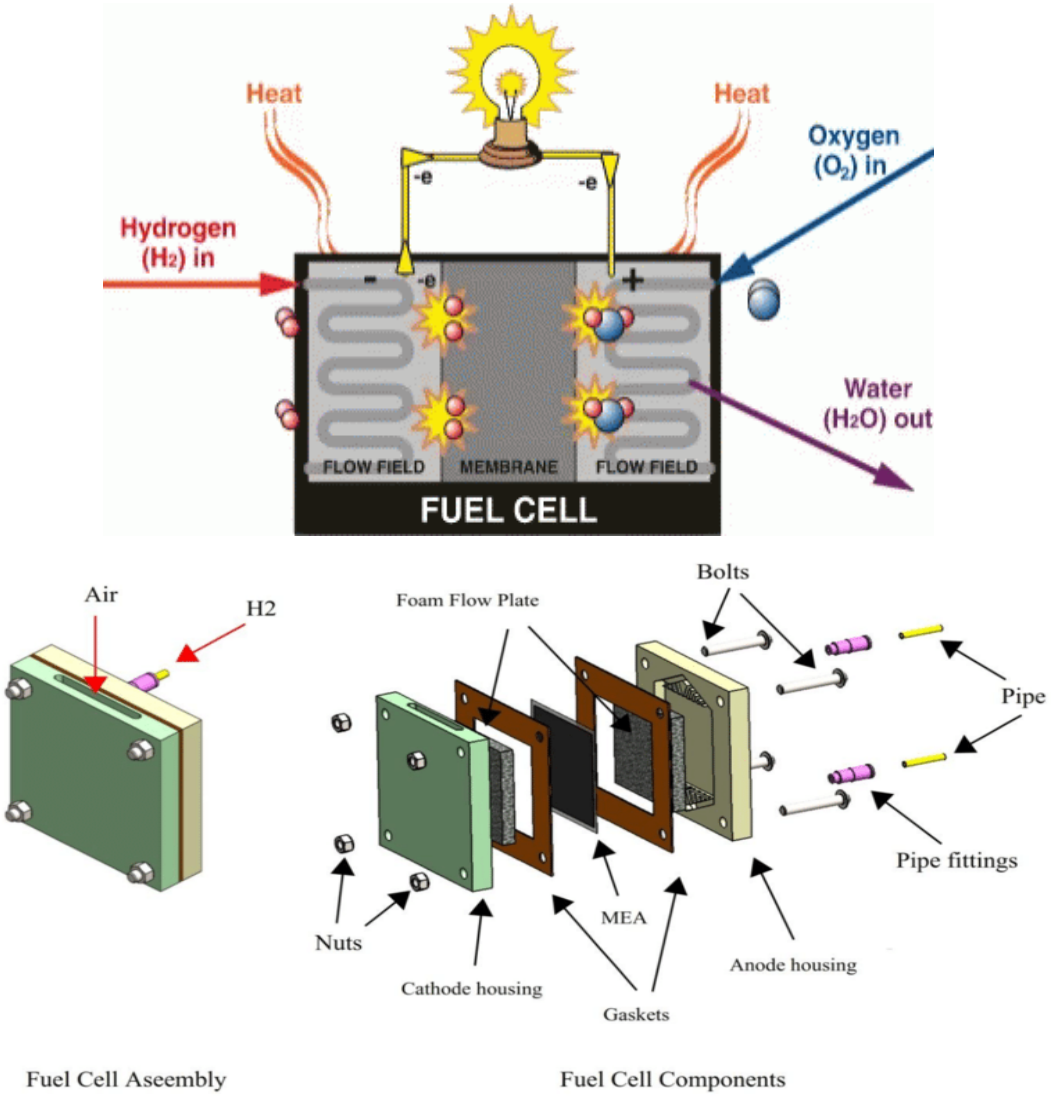

Figure 4 – Fuel cell working mechanism and different parts of the fuel cell stack [8], [9]

The fuel cell stack consists of the membrane electrode assembly (MEA), gaskets, Bipolar plates, Cooling lines, and different fittings. Overall, fuel cell reaction is exothermic; removal of the heat

and the temperature range are also necessary. Fines channels are designed to deliver the hydrogen and oxygen to the catalyst uniformly, and removal of the produced water is also essential.

2.2 ORR at Platinum surface:

Several pathways of oxygen reduction reported in the literature are shown in *figure 5* [10].

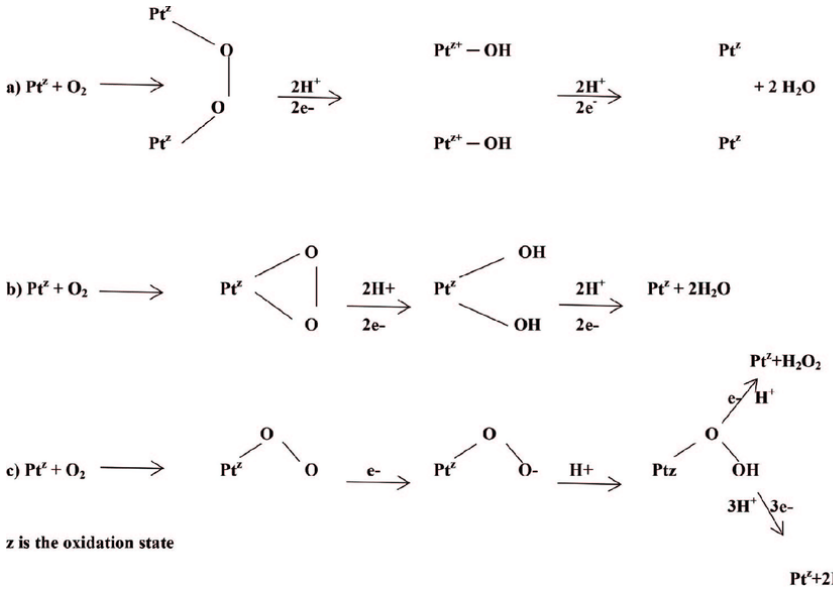

Figure 5 **–** Oxygen reduction on Pt from the (a) Bridge model, (b) Griffiths model, (c) Pauling model

As a reported mechanism, slow oxidation of the oxygen leads to hydrogen peroxide production as a by-product, which is deleterious to the carbon and affects its durability of the carbon. H2O2 may react with the carbon and lead to CO and CO_2 emissions. A suitable catalyst should be used whose surface energy promotes the bidentate oxygen adsorption on the catalyst surface to avoid hydrogen peroxide formation during the oxygen reduction reaction (ORR). Efficient catalysts follow the 4e- process in which hydrogen peroxide production does not occur. There is two proposed model which follows the 4-electron process. Among these two, the Griffiths model is the most popular and reported in the literature because of its close similarity to actual experiments with suitable catalysts.

2.3 Selection of Platinum as a catalyst:

There are many candidate metals for the ORR, but everyone has their limitations. Some have better oxygen adsorption on their surface, but -OH removal is not easy. Some have –OH removal is easy, but oxygen adsorption is not efficient. Any incoming oxygen towards the catalyst requires a suitable catalyst that easily adsorbed the oxygen on its surface. After the ORR is completed, the site should be empty for the subsequent reaction, and for that catalyst, the surface has lower surface energy to hold the reaction product. Therefore, the metal has higher surface energy for oxygen adsorption and lower surface energy to hold the –OH after the reaction. Various metal based on their adsorption of oxygen and desorption of the –OH is shown in *figure 6* [11].

Among all metals, platinum is the most promising to have both the required properties for the ORR. Since ORR is very sluggish compared to the Hydrogen Oxidation Reaction (HOR), platinum is widely used as a catalyst for the ORR in fuel cell applications. Due to the high cost of platinum, there is research for the ORR for bimetallic, polyatomic, and alloy-type catalysts.

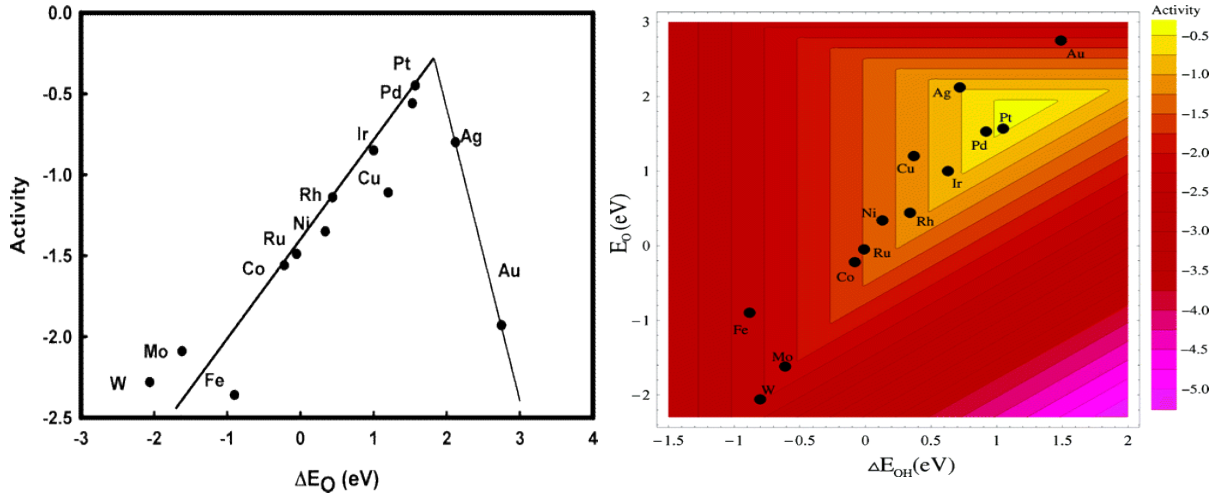

Figure 6 – (a) Oxygen reduction activity trends are shown on a graph as a function of oxygen binding energy, and (b) Plots demonstrating the patterns in oxygen reduction activity vs. the O and OH binding energies

2.4 Selection of Carbon over others supports:

Support uses for any catalyst to provide more surface area and better utilization of the small amount of the catalyst. There are different types of supports reported in the literature, such as different forms of carbons, titanium oxide (TiO_2), cerium oxide (CeO_2), tungsten oxide (WO_3), conductive polymer, zirconium carbide (ZrC), indium tin oxide (ITO), etc. Selection of the supports for fuel cell catalyst based on parameters such as -surface area & porosity, electrical conductivity, availability, cost, stability in fuel cell conditions, strong metal–support interaction, and assistance in water management. For the more extended durability of the catalyst, metal and support interaction should be firm and able to sustain in the harsh operating condition of the fuel cell.

Nowadays, water removal after the reaction is also essential to get the site for the subsequent reaction. Metal oxide has shown metal-support solid interaction and more extended durability, but more research is still required in industrial synthesis. Several efforts are taken to improve the carbon support from doping and functionalization to improve the durability of the catalyst. The cost of the supports also affects the final catalyst cost. The other available support is tabulated with their market price in *Table 2*.

Table 2 – Different supports used in the fuel cell catalyst and their market price

S. No.	Supports	Price	Supplier	Ref
1.	Carbon (Vulcan XC-72)	₹4,000/50 g	The Fuel Cell Store	[12]
2.	Carbon (Ketjen Black EC-600JD)	₹5,200/50 g	The Fuel Cell Store	[13]
3.	WO_3 (<100 nm particle size (TEM))	₹19,436.10/25 g	Sigma Aldrich	[14]
4.	TiO_2 (<100 nm particle size (TEM))	₹5,090/25 g	Sigma Aldrich	[15]
5.	CeO_2 (<50 nm particle size (TEM))	₹10,478.40/25 g	Sigma Aldrich	[16]
6.	Zirconium carbide (ZrC)	₹51,689.38/50 g	Sigma Aldrich	[17]

Due to the low price and good performance, Carbon black (VC) are more popular among researchers and industries, as VC has been reported in most literature and many industries offer Carbon-based fuel cell catalyst. So, we have taken VC as our support material. Several forms of carbon are available in the market based on their structure and porosity, as shown in *Table 3* [18] and *Table 4* [19]. The most commonly reported VC in the literature is the Vulcan carbon XC-72 (previously reported) and Ketjen Black (nowadays reported). Vulcan carbon has already been explored enough in the literature as support, and many industries accepted and used it. Therefore, we have chosen the Vulcan carbon XC-72 to support the catalyst.

Table 3 – Different supports, their suppliers, type of carbon, and BET surface area

Carbon	Supplier	Type of carbon	BET surface area ($m^2 g^{-1}$)[a]
Vulcan XC72	Cabot Corp.	Furnace black	250
Black Pearls 2000	Cabot Corp.	Furnace black	1500
Ketjen EC300J	Ketjen Black International	Furnace black	800
Ketjen EC600JD	Ketjen Black International	Furnace black	1270
Shawinigan	Chevron	Acetylene black	80
Denka black	Denka	Acetylene black	65

[a] BET: Brunauer–Emmett–Teller method.

Table 4 – Different supports and different elements contained by the XPS scan

Sample	Element (at.%)		
	Carbon	Oxygen	Sulphur
Thermal black	98.1	1.9	[a]
Furnace black	97.2	2.0	0.8
Conductex SC	99.2	0.8	[a]
Conductex 975	99.0	0.7	0.3
Printex L	99.4	0.4	0.2
Printex L6	99.6	0.2	0.2
Vulcan XC-72	99.7	[a]	0.3
Black Pearls 2000	99.8	[a]	0.2
Printex XE-2	100.0	[a]	[a]
Graphitised black	100.0	[a]	[a]

[a] Element not detected (five scans).

2.5 Carbon functionalization:

There are several problems researchers encountered during the synthesis and analysis of the catalyst: reproducibility of the electrochemical result of the same catalyst and durability of the catalyst is not as per actual life application. Many researchers reported that carbon functionalization and doping of heteroatom elements in the carbon could help to improve the carbon properties and interaction with the anchored metal and the ionomer.

Several advantages of the functionalization of carbon, such as –

- To increase the hydrophilicity of carbon
- To avoid the agglomeration of the carbon
- To enhance the better dispersion in the solvent
- Better interaction between catalyst and ionomer
- To increase the durability of the support

There are several ways of the functionalization of carbon reported in the literature. Either by the strong acid, hot hydrogen, ozone, or weak acid. As shown in *figure 7*[20], the adsorption isotherm of the platinum precursor (H_2PtCl_6) with the different chemical-treated carbon at room temperature. Pt Precursor (H_2PtCl_6) strongly interacts with weak acidity (Chloroplatinic adsorption isotherm). Weak acid anchored the high concentration of weak acid & low concentration of solid acid, which is confirmed by the Temperature Desorption Program (TDP).

Strong acid anchored the high concentration of strong acid and low concentration of the weak acid on the carbon surface.

Higher the graphitic nature:

- Lower the dispersion of the VC in the solvent
- Higher adsorption of the Pt precursor

Higher the functional groups:

- higher the dispersion of the VC in the solvent
- affect the properties of VC

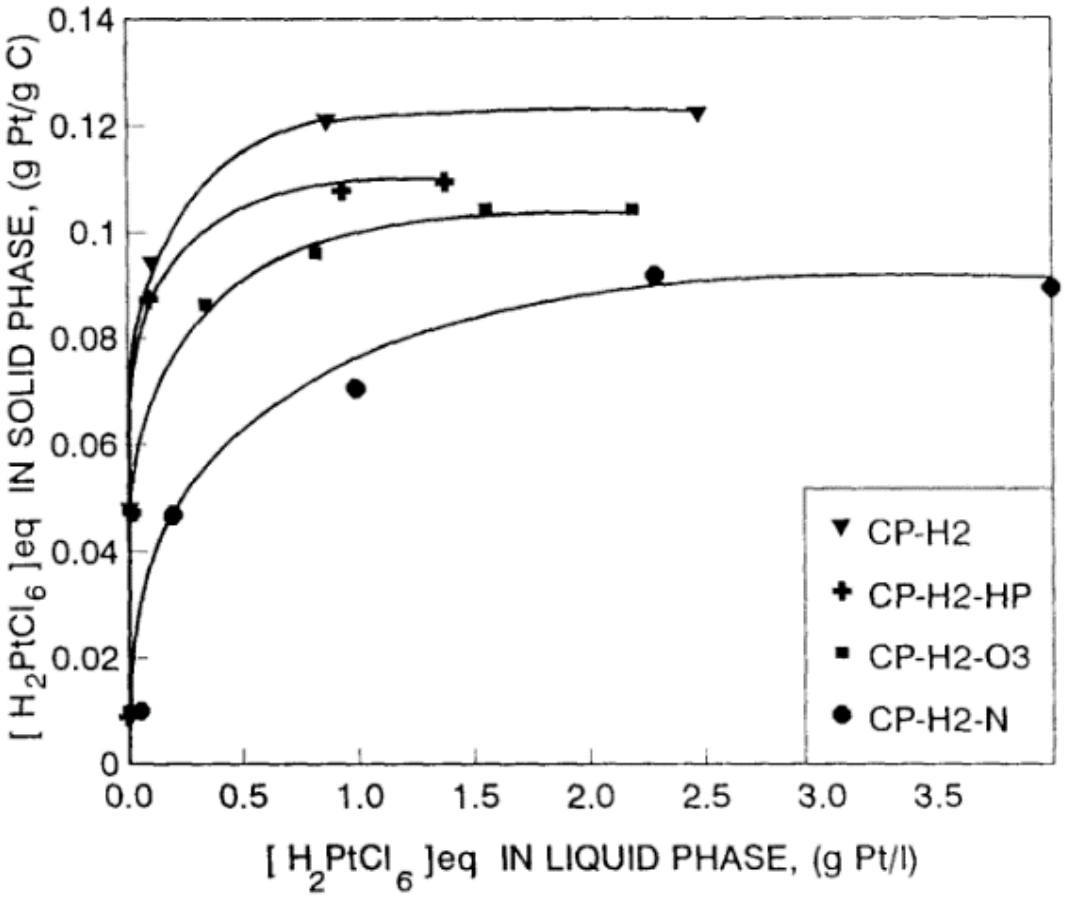

Figure 7 – H_2PtCl_6 adsorption isotherms in liquid phase at 298 K

2.6 Effect of the carbon functionalization on fuel cell operation:

Carbon black generally has sp^2 hybridization on its surface, leading to the carbon's hydrophobic nature and less interaction with the aqueous solution. Additionally, weak van der Waal force on the carbon surface leads to the agglomeration of the carbon within the solution. Cluster-formed Carbon lowered the overall surface area of the carbon and non-uniform anchoring of the Pt on the carbon surface. Therefore, functionalization of the carbon helps to overcome these problems and leads to better interaction between the ionomer and support in the fuel cell stack. As shown in *figure 8* [21], it is clearly shown that the functionalization leads to the uniform coating of the ionomer on the catalyst, which also minimizes the mass transfer limitations in the actual fuel cell conditions. Selective masking of the platinum can be done by functionalization, which helps to unmask the platinum surface and ensure the availability of the platinum surface to interact with the incoming oxygen gas [22].

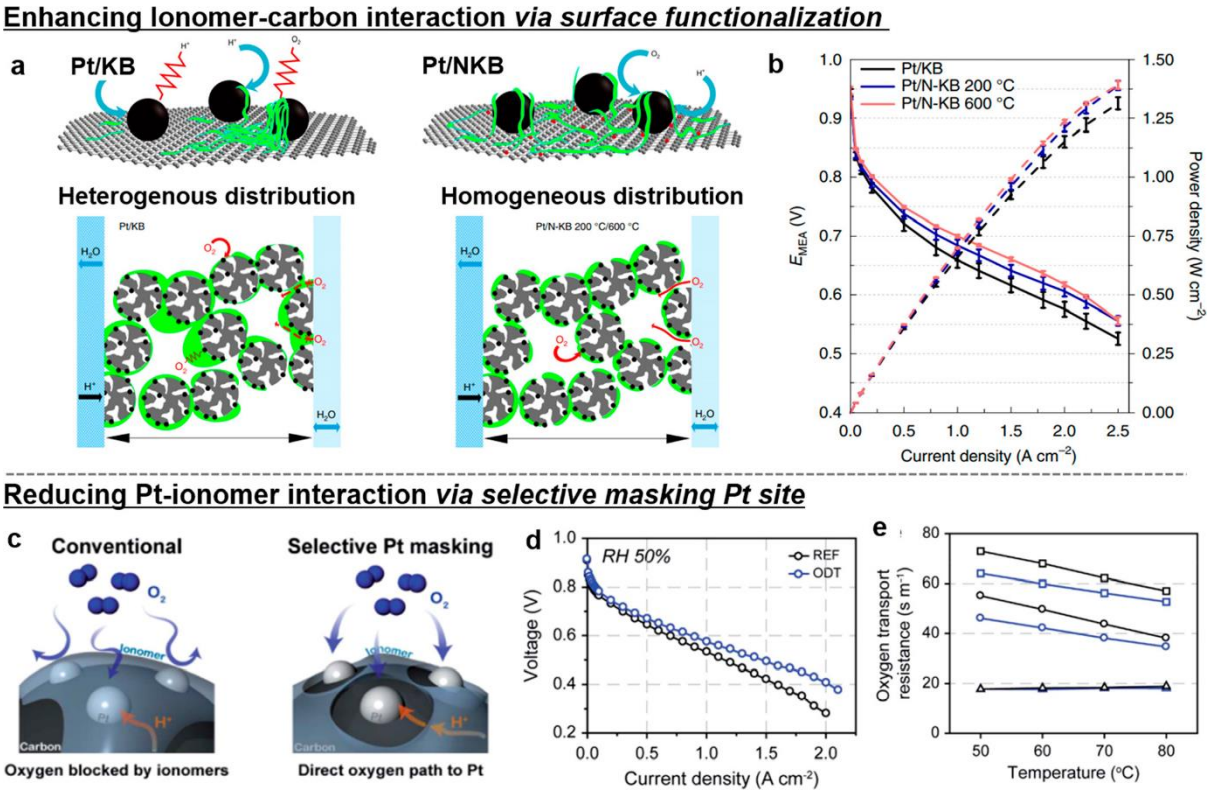

Figure 8 **–** Effect of the functionalization on the interaction of the carbon and ionomer

Functionalization has some severe limitations too. It lowers the durability of the catalyst with higher cycles. As shown in *figure 9*, we can conclude from (a) & (b) that the ECSA value drops faster in functionalized carbon compared to the pristine carbon after the accelerated degradation test (ADT). The drastic drop in the ECSA value indicates that carbon functionalization optimization is required [23]. F*igure 10* shows the reason behind the drop in the ECSA clearly. When the potential was applied, platinum interacted with oxygen (anchored by functionalization), shared an electron, and went from a lower to a higher oxidation state, leading to the accumulation of platinum on the carbon surface[23].

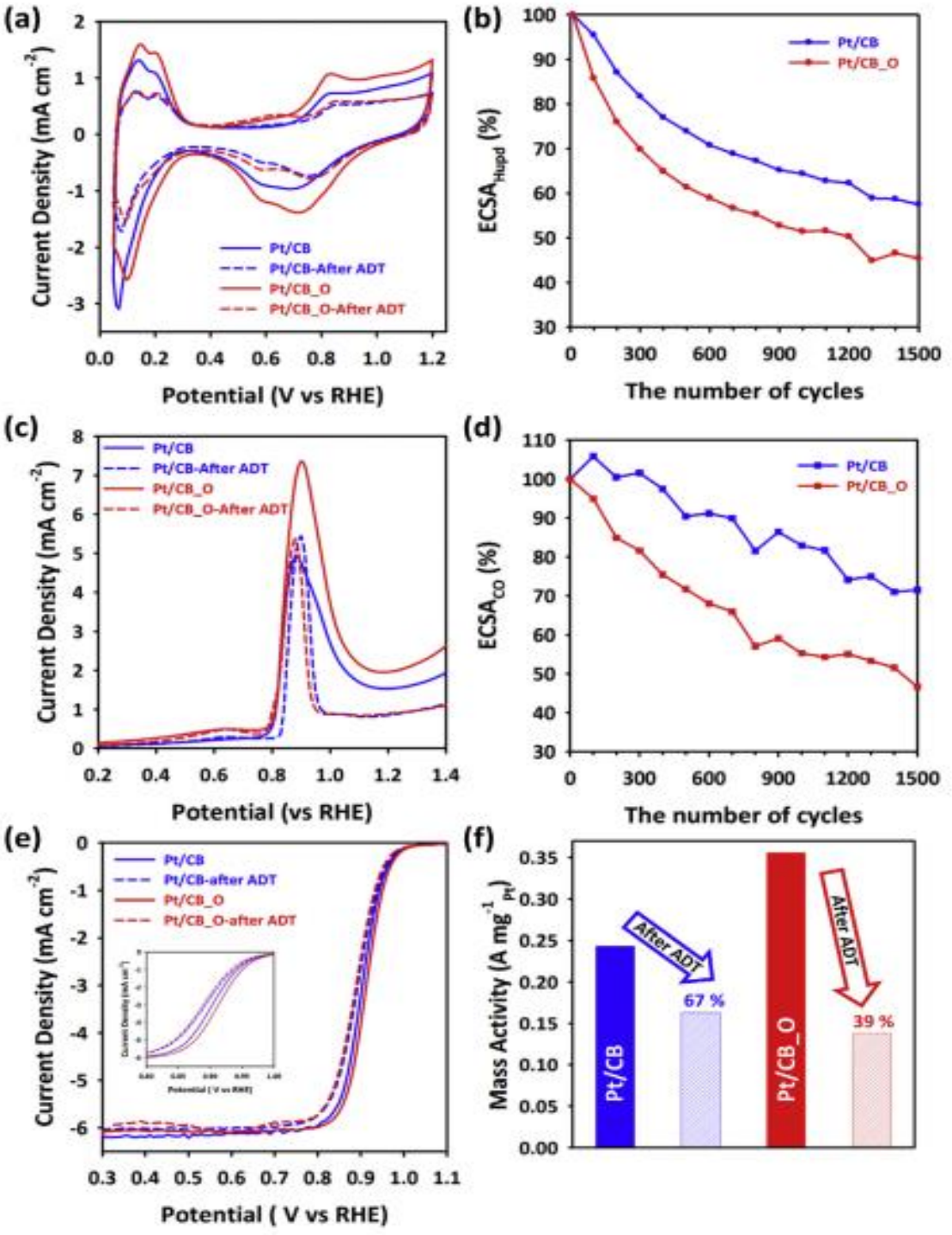

Figure 9 **–** Effect of the functionalization on the durability of the Pt/C catalyst

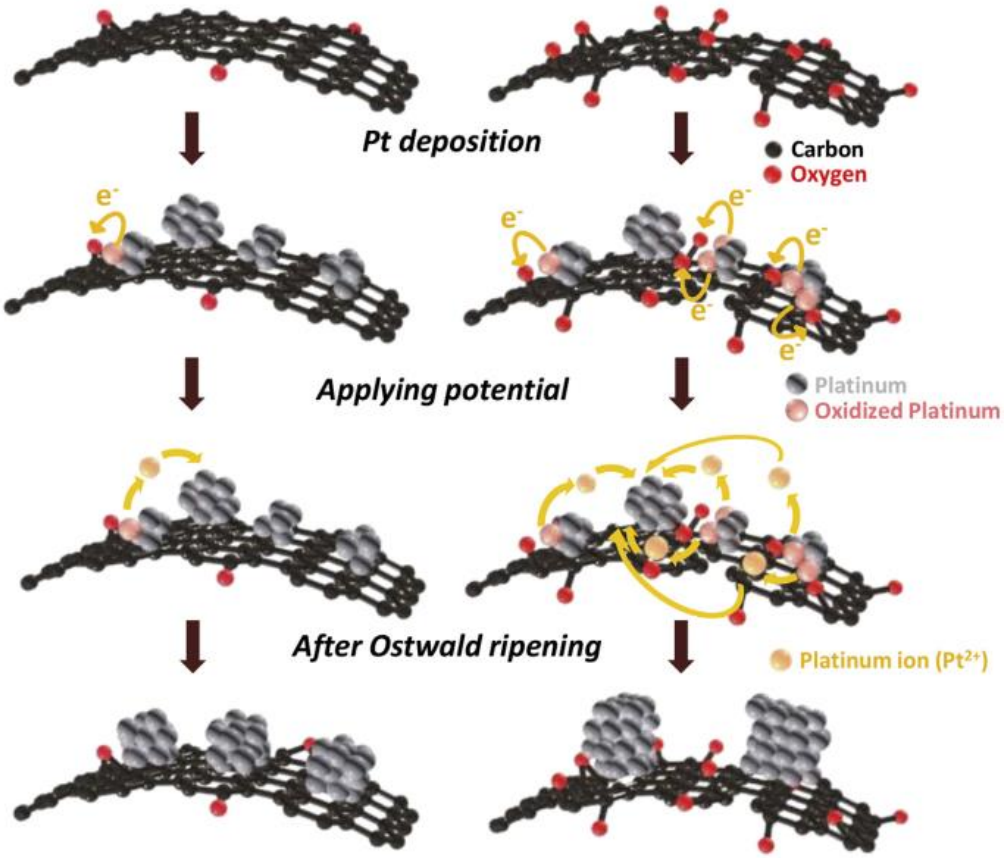

Figure 10 **–** Diagrams depicting changes in the particle size distribution of Pt before and after ADTs

2.7 Industrial Pt/C – Properties and costs:

Several industries are manufacturing Pt/C, majorly for the fuel cell application with different platinum loading on the different carbon, majorly Vulcan carbon (low surface area) and Ketjen black (high surface area). Different commercially available catalysts are tabulated in *table 5*.

Table 5 – Different commercially available Pt/C with specific properties and price

S. No.	**Name of the company**	**Catalyst**	**Pt Loading**	**Particle size (nm)**	**ECSA value (m2/g)**	**Mass activity (A/mg)**	**Durability**	**Cost**
1.	ACS Material*	Pt/C	60% Pt	3	74	0.14	ECSA loss < 40% (>**30000 cycles**)	$330/g
2.	ACS Material*	PtCu/C	40% Pt 13% Cu	4	73.2	0.25	ECSA loss < 40% (>30000 cycles)	$330/g
3.	ACS Material*	PtCu/C	50% Pt 16% Cu	4.4	83	0.435	ECSA loss < 40% (>30000 cycles)	$330/g
4.	Sigma Aldrich	Pt/C	40% Pt	<5	-	-	-	₹19,700/g
5.	Fuel Cell Etc	Pt/C	40% Pt	3-4	70	-	-	$136/g
6.	Johnson Matthey	Pt/C	40% Pt	4.5	60	-	-	-
7.	Tanaka	Pt/C	40-70* 30-50#	-	-	-	-	-

*used High surface area carbon, #used Vulcan XC72

Chapter - 3
Materials and methods

3.1 Materials –

Vulcan Carbon XC-72 was used as carbon support obtained from one of the NCL's labs. Other chemicals, Hexachloroplatinic acid (Sigma-Aldrich, 37% Pt), Ethylene Glycol (Company, Prop), DI water (Millipore Milli-Q), and H_2O_2 (Loba Chemie, Prop) used for the reaction.

3.2 Carbon functionalization –

Carbon functionalization protocols obtained from one of the NCL's labs specified the combination of VC and H_2O_2 in a ratio of 1 gm: 200 ml, a temperature of 60°C, and a reaction duration at 900 RPM magnetic stirring for 6 hours. Slow addition of the carbon into the H_2O_2 at a lower temperature. To do so, we reduce the temperature using an ice bath while stirring with a magnetic needle. More stirring time is given to moderate the slow temperature rise to prevent carbon burning because H_2O_2 is unstable at the higher temperature, converting it into water and oxygen radicals. This oxygen attacks the carbon and produces CO_2 directly. The synthesis method is shown in *figure 11*.

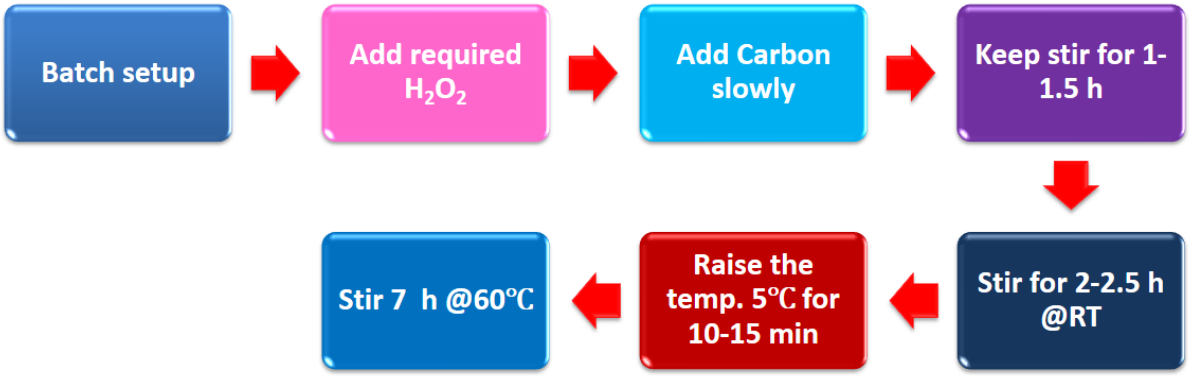

Figure 11 – Carbon functionalization method

3.3 Solvothermal (166 mg batch) –

(40 wt. % Pt/C) The solvent was first prepared using the necessary amount of 3:2 ethylene glycol and DI water. X ml of the solvent was employed for every X mg of carbon in the reaction. For a uniform dispersion, we combined 70 ml of the taken with 100 mg of the VC and sonicated it for 30 minutes. 10 ml of solvent combined with 177 mg of H2PtCl6.6H2O. After the carbon and solvent mixture had been sonicated, the precursor solution was added dropwise using the burette with the magnetic stirrer speed of 700 RPM. An additional 20 ml of the solvent was poured through the same burette to wash the adsorbed precursor on the wall. After connecting the condenser, heating is started from room temperature to 160°C. After reaching the set temperature, the reaction mixture was kept for two hours. After the reaction, let the reaction cool down to room temperature, then filter and wash with the hot DI water till no Cl- ion is detected. The product was dried at 80°C for 12 h in the dry oven.

3.4 Solvothermal (1 gm batch) –

As shown in *figure 12* – 1L jacketed baffled reactor, the magnetic needle used for the mixing, five opening in the reactor cap, two helical coiled condensers (connected by the same stream, water used as coolant), Jacketed heating (external heater used).

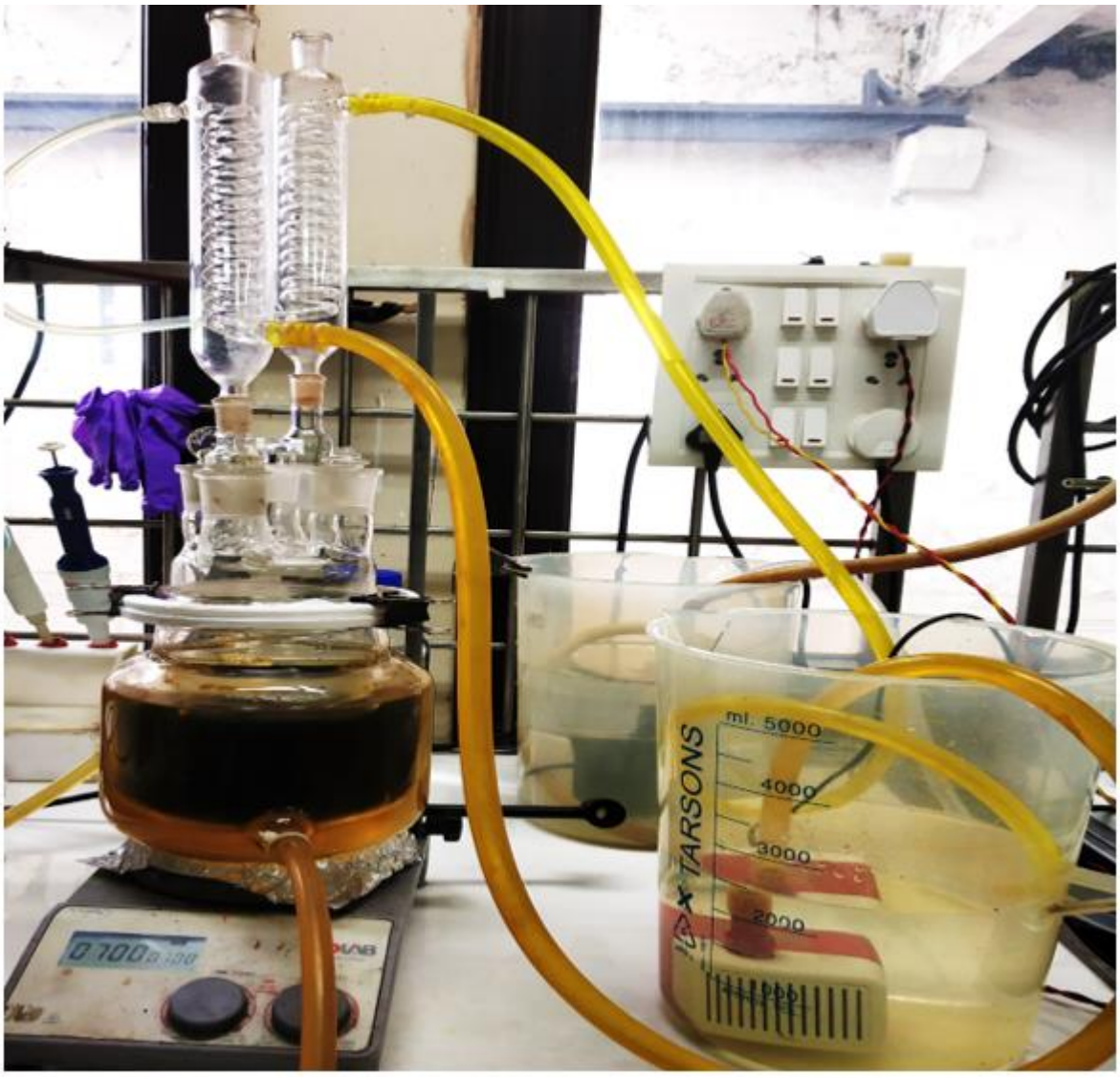

Figure 12 – Reaction setup for the 1 g batch

(40 wt. % Pt/C) The reaction procedure was almost similar to the 166 mg batch. 600 mg VC mix in the 300 ml of the solvent in the RB flask and sonicate. An Extra 100 ml was used to wash the flask after pouring the mixture into the reactor. 1062 mg of the $H_2PtCl_6.6H_2O$ mixed in 25 ml of the solvent. The precursor was added dropwise, and the rest solvent (175 ml) was added to the reactor by the same burette. After reaching 160℃, the reaction mixture was kept for heating for two h. filtered, washed, and dried the product at 80℃ for 12 h in the dry oven.

Chapter - 4
Characterization Techniques

4.1 UV-Vis Spectroscopy –

Energy received in the UV, or visible range, changes the molecule's electronic excitation, resulting in a corresponding change in its ability to absorb light in the UV-visible region of electromagnetic radiation. The smaller the energy difference between the ground and excited states, the greater the absorption wavelength would be. The position and intensity are the two main properties of an absorption band. UV-Vis spectroscopy first calibrated with the reaction solvent to eliminate the respective peaks and then utilized the particular quantity (20 µl) of the reaction sample in the reaction solvent (980 µl). Samples characterized in the range of 200-800 nm.

4.2 Field Emission Scanning Electron Microscope (FESEM):

FESEM has been used to analyze the VC more deeply and quantify the average particle size. For the sample preparation, first taken 100 µL samples in a 2 ml centrifuge tube to fill the reagent grade acetone to the 2 ml, sonicate to disperse uniformly, and then centrifuged for 30 min at 13.5 MHz. After centrifuging, remove the supernatant, add 2 ml of the same acetone, sonicate to a uniform dispersion, centrifuge, and then add 2 ml of reagent-grade ethanol. Sonicate once more to a uniform dispersion. Cast this sample on the Silicon wafer and dry under an IR lamp for 15 min.

4.3 High-Resolution Transmission Microscope (HRTEM) –

If the particle size is less than 10 nm, HRTEM gives a better imaging result than TEM. Sample preparation for the HRTEM is similar to the sample preparation of the FESEM. In contrast to the FESEM, the substrate is covered with a skinny sample layer to facilitate the electron beam's penetration. Therefore, 50 µL of the reaction sample is taken for the sample preparation rather than 100 µL as in FESEM.

Instrumentations of the HRTEM used to characterize the sample for the imagining purpose

- Model – JEM F200
- Make – JEOL
- Resolution
    - Point to point – 0.19 nm
    - TEM lattice image – 0.1 nm
    - STEM-HAADF – 0.16 nm
- Electron Gun – Schottky Field Emission Gun
- Operational voltage – 80kV and 200 kV
- CCD camera –
    - make – EMSIS
    - Model - XAROSA

4.4 Thermogravimetric Analysis (TGA)-

Thermogravimetric is used to quantify the platinum loading on the surface. Since carbon burns completely around 600°C, we take a safe range (Room temperature – 800°C) to measure the change of the weight of the sample with the temperature. We see a straight line after 600°C, indicating the platinum's weight in the sample. 5 mg of each Pt/C sample was used to characterize.

4.5 Powder X-ray diffraction (p-XRD)

A crystal produces a diffraction pattern with numerous sharp spots when an X-ray beam strikes it. These spots serve as a reflection of the crystal's periodic atomic order. When an X-ray beam lights a large number of randomly oriented crystallites found in finely powdered crystalline powder, as opposed to a single crystal, the result is that each of the spots is stretched out into a ring in the ensuing diffraction pattern. Every compound has a particular atomic order that results in an identifiable diffraction pattern. In a diffraction pattern, the ring's relative intensity and the positions each identify a specific phase of the material.

XRD was used to analyze the different facets of the platinum anchored on the carbon support. It is also used to compare the reports in the literature.

4.6 BET surface area

Brunauer-Emmett-Teller (BET) surface area analysis is a multi-point assessment of an analyte's specific surface area (m2/g) by gas adsorption analysis. An inert gas, such as nitrogen, continually flows over a given solid sample or the solid sample mixed in the gaseous volume. Weak van der Waals forces cause small gas molecules to adsorb to the solid substrate and its porous features, where they coalesce into a monolayer. Nitrogen is frequently utilized in BET surface area analysis because it is readily available in high purity and interacts strongly with most materials. In order to achieve measurable levels of adsorption, the surface is chilled using liquid N2 due to the typically poor contact between gaseous and solid phases. The nitrogen gas is then delivered into the sample cell in known quantities. By establishing circumstances of partial vacuum, it is possible to attain relative pressures lower than atmospheric pressure. No additional adsorption can occur after the saturation pressure, no matter how high the pressure is raised. Pressure fluctuations brought on by the adsorption process are monitored using highly accurate and precise pressure transducers. After the adsorption layers have formed, the sample is removed from the nitrogen environment and heated, causing the adsorbed nitrogen to be freed and quantified. The collected data is represented by a BET isotherm, which displays the quantity of gas adsorbed as a function of relative pressure. There are five different forms of adsorption isotherms.

BET surface area is used to analyze the sample's surface area and reduce with the functionalization and Platinum anchoring on the carbon support. A powder sample is used in the Nitrogen environment.

4.7 Electrochemical Half Cell

A practical and well-liked electrochemical technique called cyclic voltammetry (CV) is frequently used to study how molecular species are reduced and oxidized. CV is also crucial for researching chemical reactions catalyzed by electron transfer. CV is used to measure the current change with respect to the change of the applied voltage. This variation is depicted on the graph to analyze.

Linear Sweep Voltammetry (LSV) is a straightforward electrochemical method. The procedure is similar to cyclic voltammetry, except linear sweep voltammetry only requires a single linear sweep from the lower potential limit to the upper potential limit instead of linearly cycling through the potential range in both directions. This is especially helpful in irreversible systems where a reverse sweep would not yield any additional information. LSV has established itself as a quick and accurate characterization method that offers both qualitative and quantitative data regarding electrochemical systems. LSV has been developed for organic and inorganic synthesis, sensor and biological system evaluation, and basic physical mechanics of electron transfer reactions, such as reversibility, formal potentials, and diffusion coefficient determination. It is frequently used to study the kinetics of electron transfer reactions, including catalysis.

RDE setup and sample preparation

The three-electrode setup is used for the electrochemical analysis, as shown in *figure 13* [24]: the reference electrode, Counter electrode, and working electrode. The working electrode was a catalyst-coated glassy carbon electrode (5 mm diameter and 0.1963 cm^2 of electrode area), and the counter electrode was a graphite rod. The reference electrode was made of Ag/AgCl in saturated KCl.

The following equation calculates the electrochemical surface area (ECSA) –

$$\mathrm{ECSA} = \frac{Q_{\mathrm{H}} \times 10^2}{210 \times M_{\mathrm{Pt}}}$$

Where Q_H (C) – the charge associated with hydrogen adsorption or desorption, M_{Pt} (g) – Pt mass on the GC working electrode, and the charge associated with a hydrogen adsorption/desorption monolayer produced on smooth polycrystalline platinum averages 210 μC cm^{-2} [25].

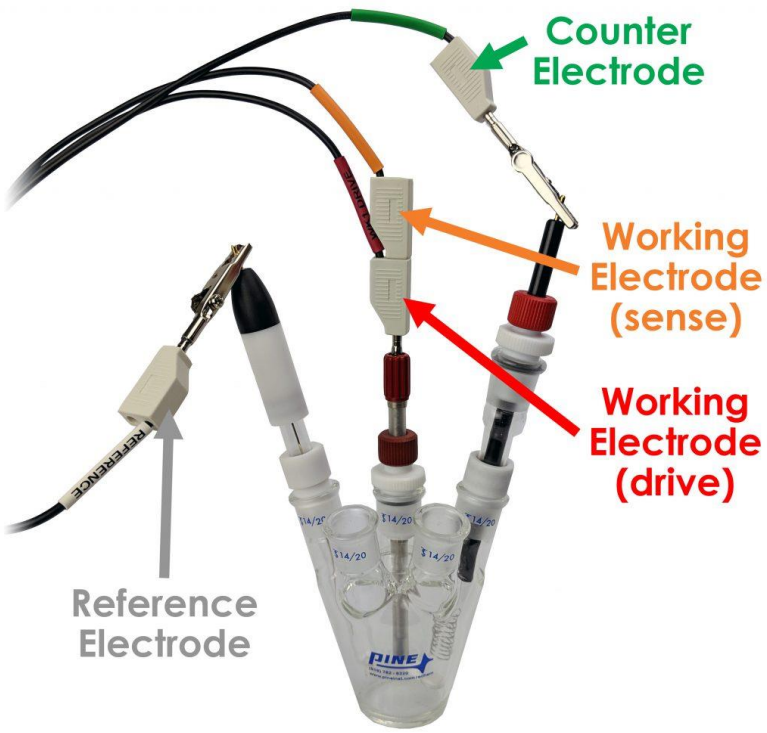

Figure 13 – Setup for the half-cell electrochemical analysis

Chapter - 5
Result and Discussion

5.1 Carbon functionalization

The carbon functionalization is done by the method stated in 3.2. According to the literature, carbon functionalization is required to enhance the interaction of carbon with an ionomer, but it also reduces the catalyst's durability in the fuel cell. Therefore, if the process is intended to go for the scale-up, quantifying the carbon functionalization is crucial to comprehend the kinetics of the process. Any decision to build up ultimately depended on the kinetic data. Three methods—FTIR, ATR-FTIR, and Boehm titration—have been tested. Standardization of the quantification approach is critical since the data received from the characterization is compared in between. Several compositions of the carbon and KBr have been experimented with to make a sufficiently transparent pellet for FTIR. Pellet preparation has yet not standardized as the pellet was opaque enough even at 1mg f-VC/250 mg of the KBr. Then, ATR-FTIR was used to characterize, but once again, there was a difficulty with method standardization. Figure 14's curve was unable to provide any quantifiable information. In the literature, Boehm titration was also mentioned as a method for determining the functional groups on the carbon surface. However, the influence of a few parameters (like stirring time and CO_2 removal) during the repeated titration produces mixed results for the same product. Therefore, each technique has limitations, and standardization is crucial for all three techniques.

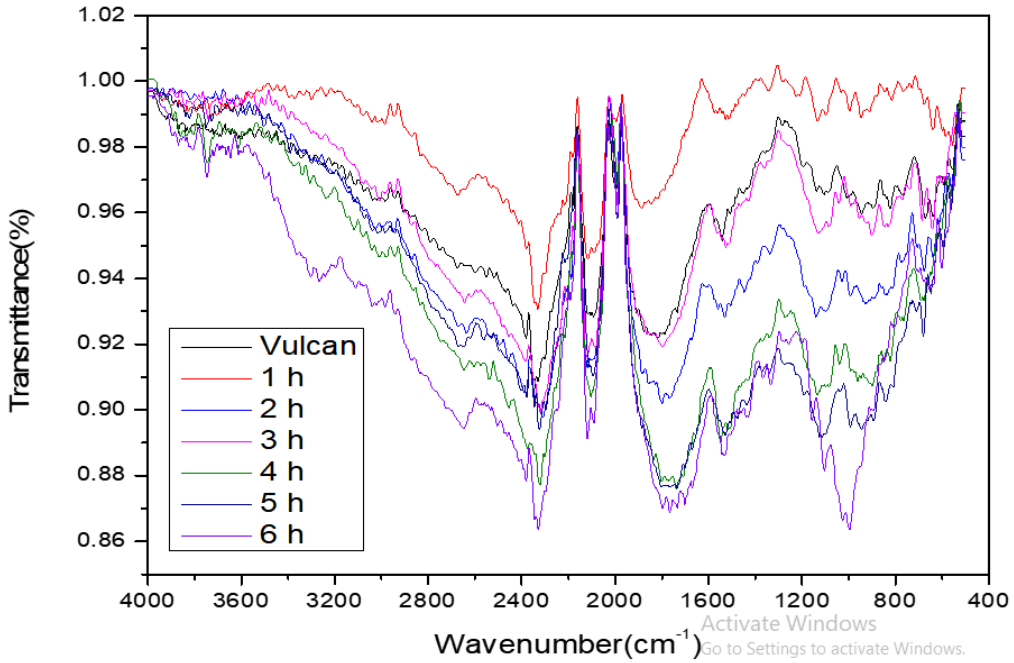

Figure 14 – ATR-FTIR result for different samples taken at different time

the as-received and functionalized VC also have seen through the optical microscope during the trial of the standardization of the technique. It has been totally opposite to the behavior reported in the literature. f-VC was expected to show less agglomeration than as-received after the functionalization, but as we can see in *figure 15*, as-received VC is less agglomerated than f-VC. To analyze further, both carbon mixed into the DI water and reaction solvent to check the dispersion and stability in the liquid [*figure 16*]. It was observed that both as-received and f-VC are stable and evenly dispersed in the reaction solvent, whereas as-received VC is more stable than

f-VC in water. After gathering data from optical microscopes and liquid dispersion, it was decided to synthesize Pt/C initially without functionalization.

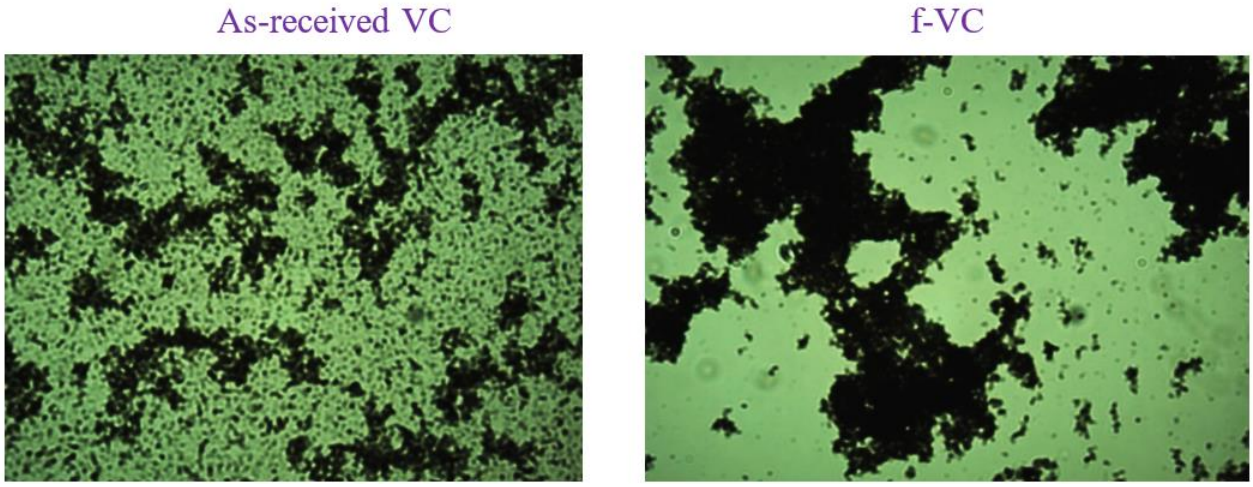

Figure 15 – Image taken from the optical microscope (100x)

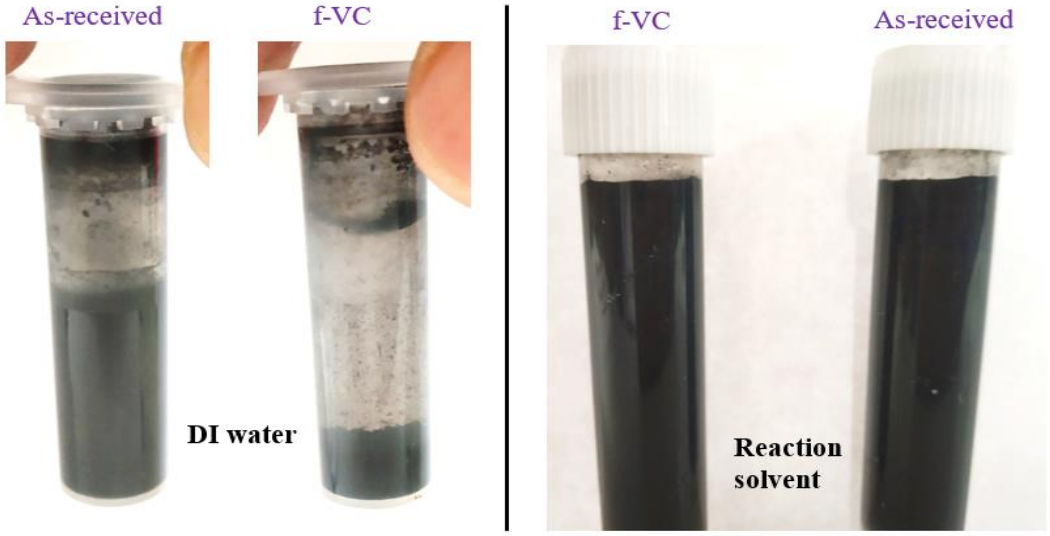

Figure 16 – Dispersion of as-received and functionalized VC in the DI water and reaction solvent; the image was taken after five days of the mixing

FESEM with imaging, EdX, and mapping was employed to analyze the carbon and its opposite behavior in more detail. The EdX result for oxygen, nitrogen, and Sulphur indicates that the matching functional groups are shown on and in the VC. The presence of nitrogen and Sulphur in carbon may be the reason for the VC's contradicting behaviors. Additionally, mapping the samples—pristine VC, functionalized VC, and Pt/pristine VC—was carried out to comprehend the distribution of the various elements in the samples, including carbon, oxygen, nitrogen, Sulphur, and platinum (only for Pt/p-VC). Any carbon already has a small number of functional groups on its surface before it is functionalized. The other carbon samples characterized platinum loading and dispersion on the carbon surface. The silicon wafer that was used to cast the sample for the FESEM testing has the most prolonged peak in Fig. (a). It dominates the other summits because it

is the most prolonged peak. The other elements are depicted in the table in Fig. (b). According to the literature, Sulphur concentrations in catalyst supports below 1% are acceptable because they do not affect the platinum negatively [need for reference]. Following the literature, nitrogen strengthens the bond between the metal and the support. It is also proven that oxygen is present. From Fig. (c), the size of the p-VC particles is close to that reported in the literature [26] at 50 nm.

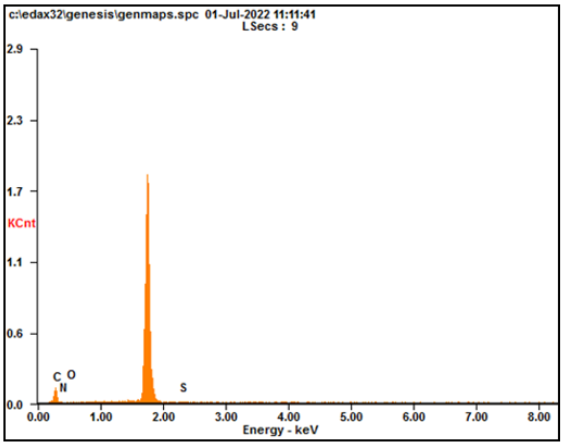

Element	Wt%	At%
CK	81.09	84.31
NK	11.16	09.95
OK	06.97	05.44
SK	00.79	00.31
Matrix	Correction	ZAF

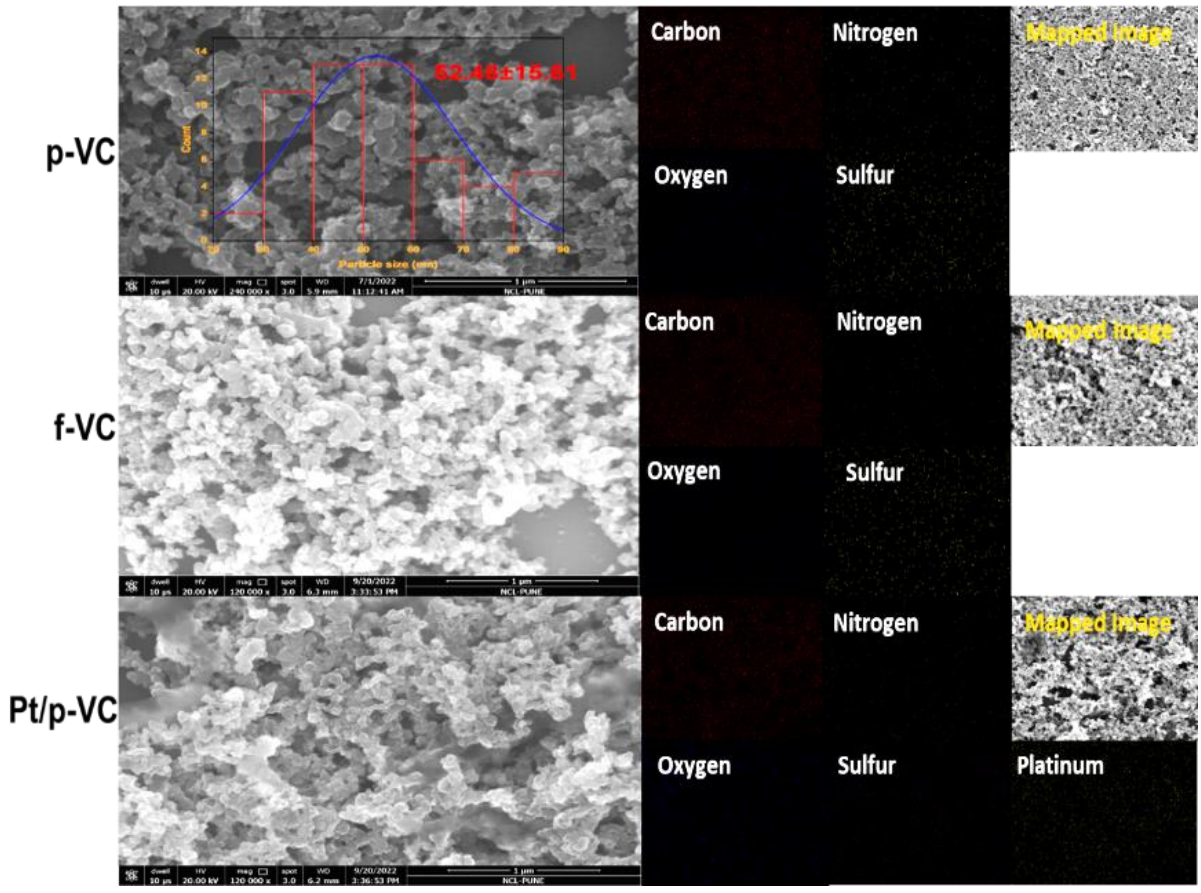

Figure 17 – FESEM data a) EdX image of pristine-VC, b) Different elements present in the pristine-VC (from EdX), and c) FESEM images and different elements mappings of the different samples

5.2 Synthesis of the Pt/VC

The catalyst Pt/C synthesize according to methods 3.3 and 3.4 for 166 mg batch and 1 gm batch. 166 mg batch was initially synthesized by 30 wt%, but all the synthesis was later done with 40 wt% Pt loading. After heating the reaction mixture, the samples were collected in different intervals and analyzed in the UV-Vis spectrometer offline. First, the reaction solvent was calibrated to eliminate the respective peaks, and then used the specific amount (20 µl) of the reaction sample in the reaction solvent (980 µl). Initially, the sample has taken in 10-minute intervals, but as shown in *figure 18* [27], the precursor had nearly substantially reduced before 20 minutes had passed since the heating began. After that, in the following reaction, The samples have taken in 2-3 min intervals. The precursor was nearly reduced in 15 minutes, according to the UV-Vis spectra; however, after 15 minutes of the reaction, the curve flattened out and did not indicate crystal nucleation or growth. It may be because of the carbon agglomeration and random charge distribution over the carbon, which separated due to the UV-Vis wave (SERS).

After the reaction, the sample is analyzed by TGA to get the Pt % loading in the catalyst. Since sample preparation is predicated on the Pt loading, it must be for the electrochemical analysis's subsequent characterization. Excellent Pt loading, at 37% in the 166 mg batch and 38% in the 1 gm batch, was demonstrated by TGA results. It might be a result of nitrogen being present in the carbon. TGA data for the 5 reproduced 166 mg and one scale-up 1 gm batch are tabulated in *table 6*.

Table 6 **-** TGA result summary of the 166 mg batch and 1 gm batch

. No.	**Experiments**	**% Pt loading**	**Average**
1	CP_Exp_04	38.55	**37.61**
2	CP_Exp_05	36.20	
3	CP_Exp_06	37.60	
4	CP_Exp_07	37.76	
5	CP_Exp_08	37.92	
6	SU_Exp_02	38.90	**38.90**

From the HRTEM data, we have excellent mean particles and particle size range as we expected to keep the particle size in the range of 2-5 nm. After analysis of 4 different reactions, we got 2.273 ± 0.464 nm average particle size from the 166 mg batch and 2.311±0.470 nm from the 1 gm batch [*Table 7*], which meant we got almost similar results after scaling up by six-fold.

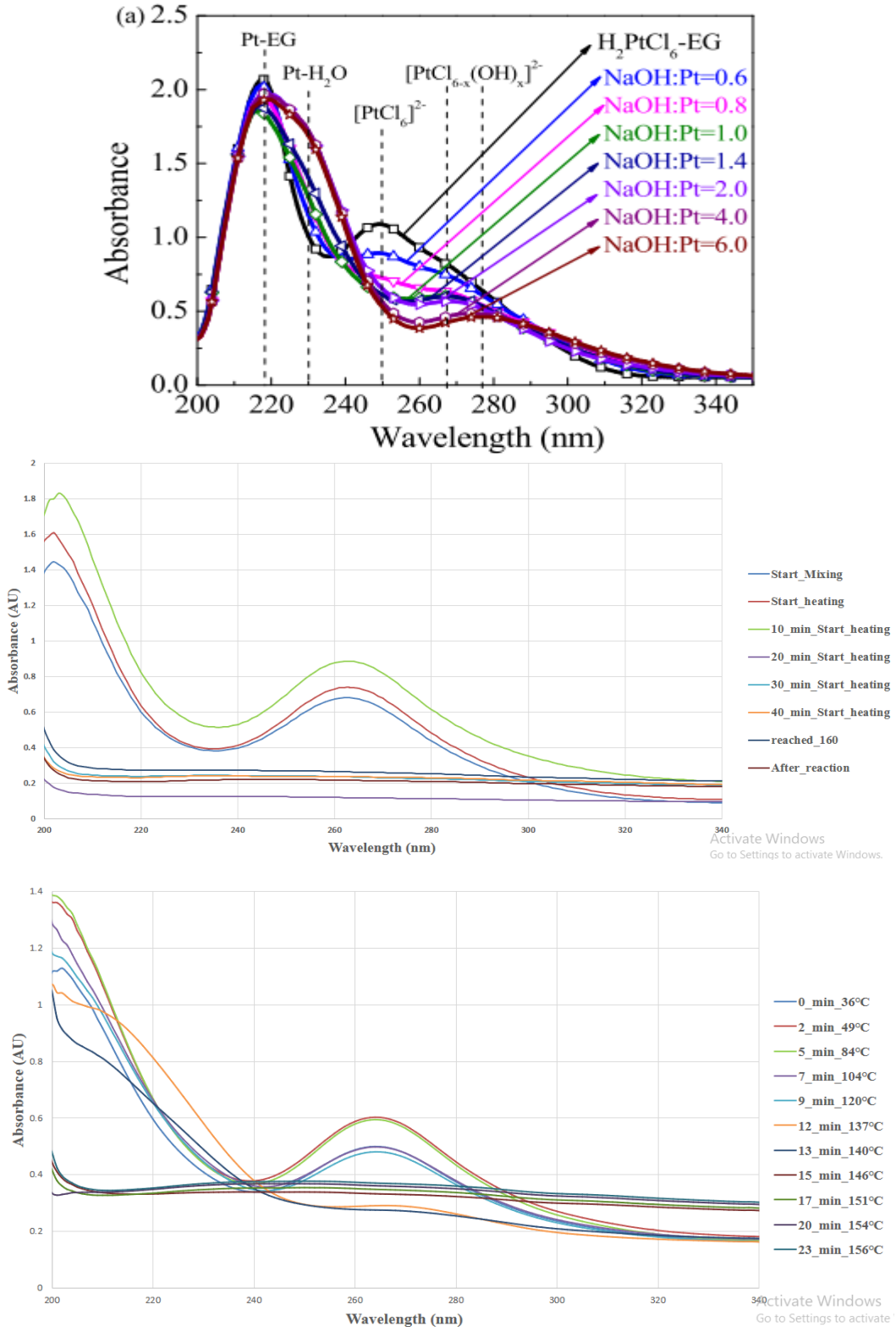

Figure 18 **–** UV-Vis spectra for different reaction time

Table 7 - HRTEM result summary of the 166 mg batch and 1 gm batch

S. No.	Experiment	Size		Standard deviation	
		Individual	**Average**	**Individual**	**Average**
1	CP_Exp_04	2.217		0.500	
2	CP_Exp_05	2.124		0.404	
3	CP_Exp_06	2.565	**2.273**	0.481	**0.464**
4	CP_Exp_07	2.188		0.472	
5	CP_Exp_08	-		-	
6	SU_Exp_02	2.311	**2.311**	0.47	**0.470**

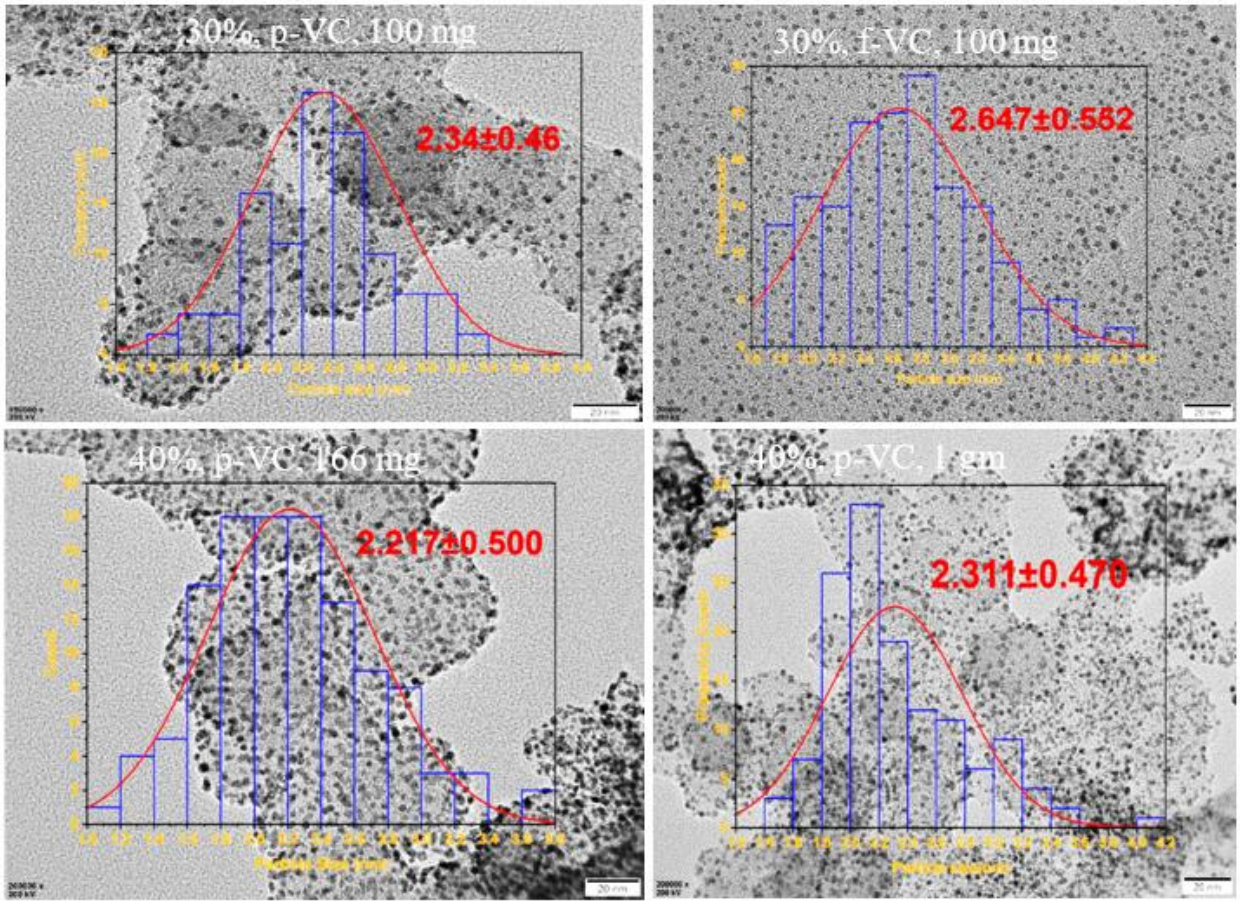

Figure 19 - HRTEM result summary of the 166 mg batch and 1 gm batch

The XRD result showed that the excellent dispersion and crystal facet are similar to the literature reported [*figure 20*].

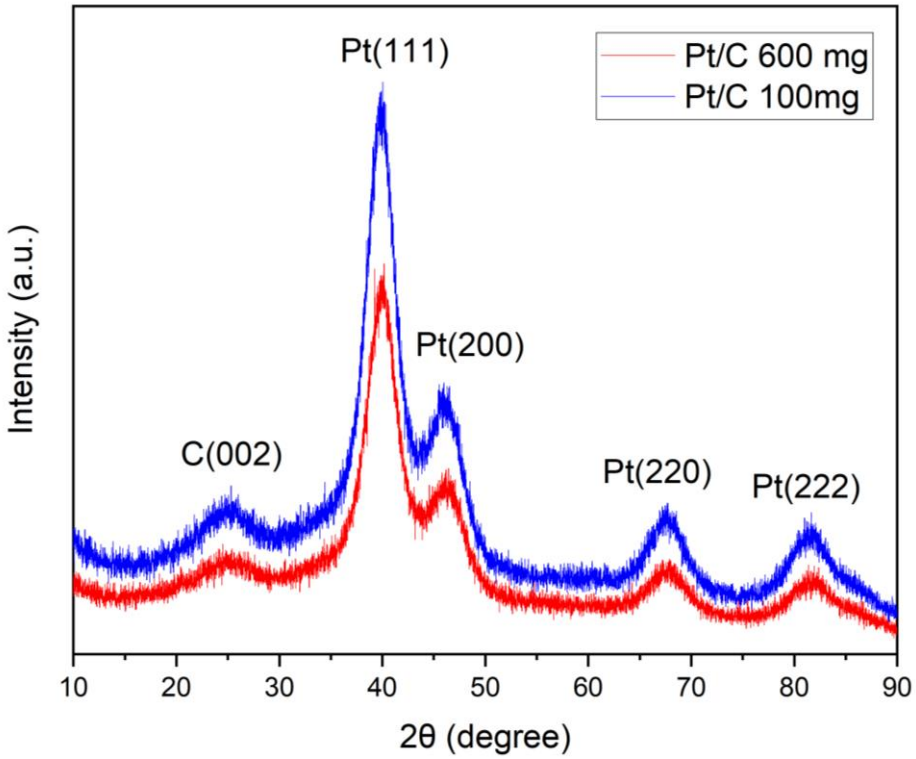

Figure 20 **–** XRD result of the 166 mg batch and 1 gm batch

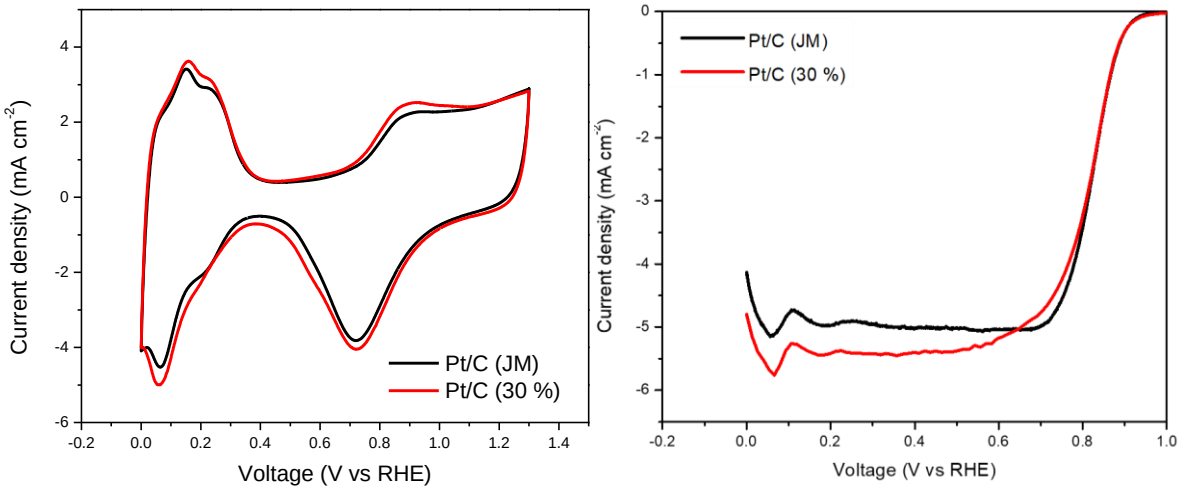

Figure 21 **–** CV and LSV result for the 30 wt% Pt/C

As said earlier, 30 wt % Pt/C was synthesized initially, and after the TGA result, the electrochemical analysis has done. For the comparison, the Johnson Matthey catalyst was used. The condition for the analysis was N_2 sat. CV at 0 rpm 50mV scan rate 0.1M $HClO_4$ solution. We have ECSA value Pt/C (30 %) – 60 $m^2/g_{Pt,}$ whereas JM catalyst had 64 m^2/g_{Pt}.

After a 30 wt % Pt/C batch, the 40 wt % Pt/C was synthesized in a 166 mg batch. Compared to the 30 wt % Pt/C, 30 wt % Pt/C gave an exciting result. The electrochemical result has shown 74.32 m2/g_{Pt} from the 40 wt % Pt/C, whereas JM catalysts have 58.33 m^2/g_{Pt} for the same loading. After getting a pretty good result, it was decided to repeat the same reaction procedure five times to verify its reproducibility. The repeated reactions also gave almost the same result as the TGA and HRTEM results. Electrochemical analysis was done for the two reactions' final samples, which were almost close to each other. As per the 166 mg batch, repeated experiments gave close results to each other, and it was decided to move to scale up for a 1 gm batch. The complete fuel cell analysis required more than 500 mg of the catalyst. The complete cell analysis gives the actual ECSA value and durability in the fuel cell's operating condition. Therefore, the same reaction conditions kept synthesizing the 1 gm 40 wt% Pt/C batch (SU_Exp_02). The setup and reaction procedure were explained in section 3.4. The TGA, HRTEM, XRD, and Electrochemical results have been in the Table, Table, Table, and Figure, respectively. ECSA value for the electrochemical analysis was 70.48 m^2/g_{Pt}, close to the 166 mg batch.

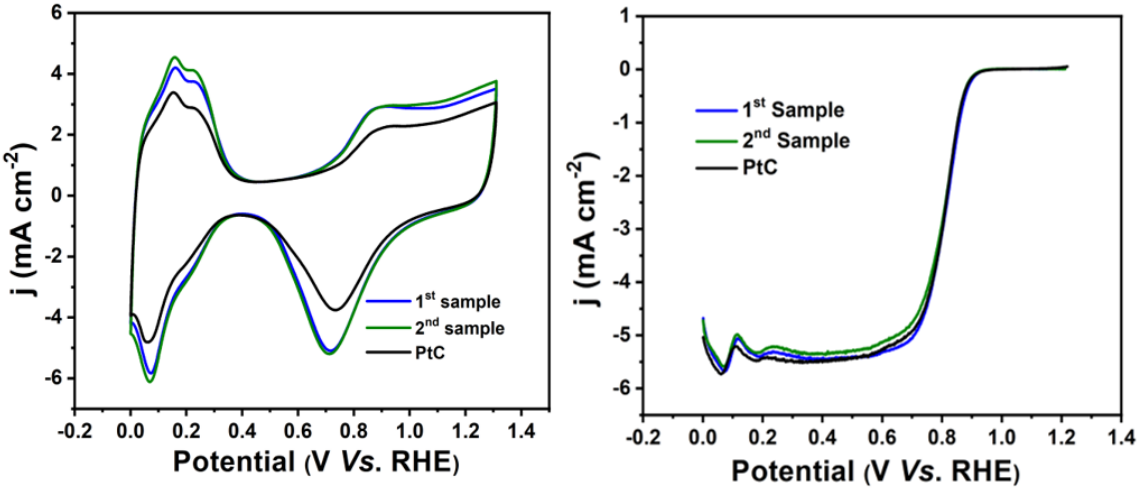

Figure 22 – CV and LSV result for the 40 wt% Pt/C

Condition:
Pt/C JM O_2 sat. nitrogen corrected LSV at 1600 rpm at 10mV scan rate 0.1M $HClO_4$ solution

Half-cell study
0.1M $HClO_4$ medium
LSV at 10mVs^{-1} O_2 atmosphere
Onset = 0.91V (for all)
Half wave Pot. = 0.81V (for all)
Lim. Current = -5.6mA (+/- 0.2mAcm^{-2} error bar)

Half-cell study
0.1M $HClO_4$ medium
CV at 50mVs^{-1} N_2 atmosphere
ECSA Pt/C JM = 58.33 $m^2 mg_{pt}^{-1}$
ECSA 1st sample= 74.32$m^2 mg_{pt}^{-1}$
ECSA 2nd sample= 76.58 $m^2 mg_{pt}^{-1}$

Figure 23 – Electrochemical analysis (CV and LSV) conditions and result for 40wt% Pt/C

BET surface area, Total pore volume, and Average pore radius of the as-received VC, functionalized-VC, Pt/C of the 166 batches, and Pt/C of the 1 gm batch are tabulated in *table 8*. Pt/C from both the 166 mg batch and 1 gm batch has almost similar BET results, showing the batches' excellent reproducibility.

Table 8 **–** BET surface area, Average pore radius, and Total pore volume

S. No.	Experiments	Surface area, m^2/g	Total pore volume, cc/g	Average pore radius, Å
1	Vulcan Carbon XC-72	218.486	1.51E+00	1.22E+02
2	CT_Exp_04	154.306	1.41E+00	1.63E+02
3	CP_Exp_06	144.116	9.97E-01	1.17E+02
4	SU_Exp_02	140.979	8.16E-01	9.92E+01

Conclusions –

With good interaction with the ionomers and uniform coating throughout, functionalization of the carbon support contributes to better results and lessens the mass transfer constraints during the ORR. According to the literature review, functionalization also aids in durability. The functional groups attached to the carbon following functionalization were also measured. The standardizations of the measurement procedure were confronted when using Boehm titration, FTIR, and ATR-FTIR. An in-depth literature review is required to standardize the process. The dispersion and stability have evaluated functionalized and as-received carbon in both water and the reaction solvent. It was found that the carbon in the latter had good stability and dispersion.

For the 40 wt% Pt/C synthesis –

- 100 mg batch of the catalyst has reproduced five times
- The almost similar result from the 600 mg batch
- BET surface area shows a similar result for the 166 mg batcha and 1 gm batch
- Average Pt particle size ~ 2.2 nm for the
- ~38% platinum loading on the carbon (TGA)
- ~99% conversion and ~95% selectivity from both batch
- XRD result shows almost similar dispersion in both batch
- Half-cell analysis shows the ECSA value
  - 75.~ m^2/g (166 mg batch)
  - 70.5 m^2/g (1 gm batch)

Future Outlook –

- Reproducibility of the 1 gm batch
- Durability test of the 1 gm batch catalyst
- Convert batch into the flow
- Optimization of the Reaction time, temperature
- Kinetic study of the process
- A thorough literature review is also necessary to quantify the functional groups anchored by carbon functionalization
- The viability of using the Inline-FTIR to achieve the same goal must be examined
- The functionalization's impact on the fuel cell's catalyst durability must then be evaluated

References –

[1] "National Hydrogen Mission launched | India News,The Indian Express." https://indianexpress.com/article/india/from-ioc-to-reliance-indias-hydrogen-push-gains-traction-7454869/ (accessed Oct. 28, 2022).

[2] "Each Country's Share of CO2 Emissions | Union of Concerned Scientists." https://www.ucsusa.org/resources/each-countrys-share-co2-emissions (accessed Oct. 28, 2022).

[3] "How are the poor impacted by climate change?" https://skepticalscience.com/co2-limits-poor-poverty.htm (accessed Oct. 28, 2022).

[4] "Climate Change Mitigation: Role of Social Cost of Carbon - Alliance for an Energy Efficient Economy." https://aeee.in/climate-change-mitigation-role-of-social-cost-of-carbon/ (accessed Oct. 28, 2022).

[5] H. S. Das, M. F. F. Chowdhury, S. Li, and C. W. Tan, "Fuel cell and hydrogen power plants," *Hybrid Renew. Energy Syst. Microgrids*, pp. 313–349, Jan. 2021, doi: 10.1016/B978-0-12-821724-5.00009-X.

[6] S. T. Thompson *et al.*, "Direct hydrogen fuel cell electric vehicle cost analysis: System and high-volume manufacturing description, validation, and outlook," *J. Power Sources*, vol. 399, pp. 304–313, Sep. 2018, doi: 10.1016/J.JPOWSOUR.2018.07.100.

[7] "Electrochemistry Encyclopedia – PEM fuel cells." https://knowledge.electrochem.org/encycl/art-f04-fuel-cells-pem.htm (accessed Oct. 28, 2022).

[8] "Hydrogen Fuel GIF - Hydrogen Fuel Cell - Discover & Share GIFs." https://tenor.com/view/hydrogen-fuel-cell-gif-7238869 (accessed Oct. 28, 2022).

[9] A. Baroutaji, J. G. Carton, J. Stokes, and A. G. Olabi, "Design and development of proton exchange membrane fuel cell using open pore cellular foam as flow plate material," 2014.

[10] A. Ray, I. Mukhopadhyay, R. K. Pati, and L. Khotseng, "Electrocatalysts for Fuel Cells and Hydrogen Evolution - Theory to Design," *Electrocatal. Fuel Cells Hydrog. Evol. - Theory to Des.*, Dec. 2018, doi: 10.5772/INTECHOPEN.72563.

[11] J. K. Nørskov *et al.*, "Origin of the overpotential for oxygen reduction at a fuel-cell cathode," *J. Phys. Chem. B*, vol. 108, no. 46, pp. 17886–17892, Nov. 2004, doi: 10.1021/JP047349J/ASSET/IMAGES/LARGE/JP047349JF00008.JPEG.

[12] "Carbon Black - Vulcan XC 72R." https://www.fuelcellstore.com/vulcan-xc-72r (accessed Oct. 28, 2022).

[13] "Carbon Black - Ketjenblack EC-600JD." https://www.fuelcellstore.com/ketjenblack-carbon-black-ec600jd (accessed Oct. 28, 2022).

[14] "Tungsten(VI) oxide - Tungstic anhydride."

https://www.sigmaaldrich.com/IN/en/substance/tungstenvioxide231841314358 (accessed Oct. 28, 2022).

[15] "Titanium(IV) oxide, mixture of rutile and anatase - Titanium dioxide." https://www.sigmaaldrich.com/IN/en/substance/titaniumivoxidemixtureofrutileandanatase798713463677 (accessed Oct. 29, 2022).

[16] "Cerium(IV) oxide - Ceric oxide, Ceric oxide." https://www.sigmaaldrich.com/IN/en/substance/ceriumivoxide172111306383 (accessed Oct. 29, 2022).

[17] "Zirconium carbide -." https://www.sigmaaldrich.com/IN/en/substance/zirconiumcarbide1234598765 (accessed Oct. 29, 2022).

[18] X. Yu and S. Ye, "Recent advances in activity and durability enhancement of Pt/C catalytic cathode in PEMFC: Part I. Physico-chemical and electronic interaction between Pt and carbon support, and activity enhancement of Pt/C catalyst," *J. Power Sources*, vol. 172, no. 1, pp. 133–144, Oct. 2007, doi: 10.1016/J.JPOWSOUR.2007.07.049.

[19] D. Pantea, H. Darmstadt, S. Kaliaguine, and C. Roy, "Electrical conductivity of conductive carbon blacks: influence of surface chemistry and topology," *Appl. Surf. Sci.*, vol. 217, no. 1–4, pp. 181–193, Jul. 2003, doi: 10.1016/S0169-4332(03)00550-6.

[20] G. C. Torres *et al.*, "Effect of the carbon pre-treatment on the properties and performance for nitrobenzene hydrogenation of Pt/C catalysts," *Appl. Catal. A Gen.*, vol. 161, no. 1–2, pp. 213–226, 1997, doi: 10.1016/S0926-860X(97)00071-9.

[21] G. Doo *et al.*, "Nano-scale control of the ionomer distribution by molecular masking of the Pt surface in PEMFCs," *J. Mater. Chem. A*, vol. 8, no. 26, pp. 13004–13013, Jul. 2020, doi: 10.1039/C9TA14002F.

[22] S. Ott *et al.*, "Ionomer distribution control in porous carbon-supported catalyst layers for high-power and low Pt-loaded proton exchange membrane fuel cells," *Nat. Mater. 2019 191*, vol. 19, no. 1, pp. 77–85, Sep. 2019, doi: 10.1038/s41563-019-0487-0.

[23] J. H. Kim, J. Y. Cheon, T. J. Shin, J. Y. Park, and S. H. Joo, "Effect of surface oxygen functionalization of carbon support on the activity and durability of Pt/C catalysts for the oxygen reduction reaction," *Carbon N. Y.*, vol. 101, pp. 449–457, May 2016, doi: 10.1016/J.CARBON.2016.02.014.

[24] "Three-Electrode Setups – Pine Research Instrumentation Store." https://pineresearch.com/shop/kb/applications/rde-and-rrde/three-electrode-setups/ (accessed Oct. 29, 2022).

[25] K. Yoshii *et al.*, "Highly durable Pt nanoparticle-supported carbon catalysts for the oxygen reduction reaction tailored by using an ionic liquid thin layer," *J. Mater. Chem. A*, vol. 4, no. 31, pp. 12152–12157, Aug. 2016, doi: 10.1039/C6TA04859E.

[26] Q. Wei, X. Tong, G. Zhang, J. Qiao, Q. Gong, and S. Sun, "Nitrogen-Doped Carbon Nanotube and Graphene Materials for Oxygen Reduction Reactions," *Catal. 2015, Vol. 5, Pages 1574-1602*, vol. 5, no. 3, pp. 1574–1602, Sep. 2015, doi: 10.3390/CATAL5031574.

[27] R. Zeng, K. Wang, W. Shao, J. Lai, S. Song, and Y. Wang, "Investigation on the coordination mechanism of Pt-containing species and qualification of the alkaline content during Pt/C preparation via a solvothermal polyol method," *Chinese J. Catal.*, vol. 41, no. 5, pp. 820–829, 2020, doi: 10.1016/S1872-2067(19)63456-X.